

ARTICLE

OPEN



The power of microscopic nonclassical states to amplify the precision of macroscopic optical metrology

Wenchao Ge ^{1,2,3}✉, Kurt Jacobs ^{4,5}✉ and M. Suhail Zubairy ³

It is well-known that the precision of a phase measurement with a Mach-Zehnder interferometer employing strong classic light can be greatly enhanced with the addition of weak nonclassical light. In the context of quantifying nonclassicality, the amount by which a nonclassical state can enhance precision in this way has been termed its 'metrological power'. To-date, the enhancement provided by weak nonclassical states has been calculated only for specific measurement configurations. Here we are able to optimize over all measurement configurations to obtain the maximum enhancement that can be achieved by any single or multi-mode nonclassical state together with strong classical states, for local and distributed quantum metrology employing any linear or nonlinear single-mode unitary transformation. Our analysis reveals that the quantum Fisher information for quadrature-displacement sensing is the sole property that determines the maximum achievable enhancement in all of these different scenarios, providing a unified quantification of the metrological power.

npj Quantum Information (2023)9:5 ; <https://doi.org/10.1038/s41534-022-00670-9>

INTRODUCTION

Measurement devices that employ quantum systems in nonclassical states can outperform their classical counterparts using no more resources. The resources here are the number, N , of photons, phonons, spin-1/2 systems, or other elementary probe systems used by the device^{1–12}. The precision of classical devices scales at most with the square root of N , whereas that of quantum devices can in principle scale linearly with N , a scaling referred to as the Heisenberg limit³. Recent studies have tended to focus on the use of quantum systems to achieve this optimal scaling. However, as pointed out by Lang and Caves¹³, since nonclassical states become harder to produce the larger N , for measurements using light, even weak lasers will outperform the most energetic nonclassical states produced to-date, something that is likely to remain true for the foreseeable future.

Even with the above limitation, nonclassical states of light are remarkably powerful: few-photon nonclassical states can greatly enhance the precision of measurements that employ classical states with 10^{12} photons¹⁴. A well-known example is that of a Mach-Zehnder interferometer (MZI)^{4,13,15–18}. A coherent state with N_c photons injected into one input of the MZI achieves a precision for phase measurement of $\mathcal{P} = \sqrt{N_c}$ ⁴. (The precision is defined here as the inverse of the minimum measurement error—see below.) Injecting a squeezed state with N_q photons into the second input of the MZI increases this precision to approximately $\sqrt{4N_qN_c}$ ^{4,13,15,16}. Thus to achieve a given precision, the addition of only 2.5 nonclassical photons reduces the required power of the classical input by an order of magnitude, while 25 nonclassical photons reduces it by two orders of magnitude.

The ability of nonclassical states to perform metrology is an important element in the study of nonclassicality as a resource^{16,19–21}. For this purpose classical resources are free, so the quantity of interest is the amount by which nonclassical states increase precision when employed with arbitrarily large coherent

states, the same limit in which we are interested in practical purposes. This quantity has been termed the metrological power, $\mathcal{M}_{\hat{\rho}}$, of a nonclassical state, $\hat{\rho}$ ²¹. It provides a resource theoretic measure of nonclassicality for pure states and a witness of nonclassicality for mixed states^{16,20,21}.

The enhancement to otherwise classical measurements provided by weak nonclassical states has been calculated for specific scenarios such as the MZI, but the maximal enhancement enabled by any given state (that is, the metrological power) and how to achieve it has remained lacking. Here we answer these questions for all nonclassical states of light and for both local and distributed quantum metrology^{22–27}. The latter involves estimating a linear combination of a number of independent values of the same physical quantity^{28–30}. Since the quantities of interest for metrology to date have invariably been transformations of individual modes (e.g., displacement and phase shifts) we restrict ourselves to unitary transformations of a single mode here, obtaining results for all such transformations, including linear and nonlinear³¹, for which the metrological power is well-defined.

A summary of our main results is as follows. First, we show that the quantum enhancement is always proportional to the classical precision, so this enhancement is always an amplification of the classical precision. Second, the metrological power for the metrology of every single-mode transformation is determined by a single quantity. For single-mode states, this quantity is the quantum Fisher information (QFI) for measuring phase-space displacement using that state. For pure states, this QFI reduces to the maximum quadrature variance for the mode. For multi-mode states, it is the same quantity but this time evaluated for the linear combination of the modes for which this QFI is the largest.

We show that for a single-mode nonclassical state and strong coherent state(s), the maximum precision can be obtained for single-parameter estimation merely by displacing the mode by the total available classical amplitude. For two-parameter

¹Department of Physics, University of Rhode Island, Kingston, RI 02881, USA. ²Department of Physics, Southern Illinois University, Carbondale, IL 62901, USA. ³Institute for Quantum Science and Engineering (IQSE) and Department of Physics and Astronomy, Texas A&M University, College Station, TX 77843-4242, USA. ⁴United States Army Research Laboratory, Adelphi, MD 20783, USA. ⁵Department of Physics, University of Massachusetts at Boston, Boston, MA 02125, USA. email: wenchaoe.tamu@gmail.com; dr.kurt.jacobs@gmail.com

distributed quantum metrology the balanced MZI achieves the maximum precision. For a multi-mode nonclassical state, the maximum precision can be obtained by first employing a linear network that outputs the linear combination of the modes into a single mode that has the largest QFI for displacement measurement, and then using this mode as the nonclassical input to the optimal schemes employing single-mode nonclassical states.

Moreover, since squeezed vacuum states have the minimum energy for a given value of the quadrature variance, our results imply that a squeezed vacuum is the most energy efficient among single-mode nonclassical states for amplifying the precision for metrology of any single-mode transformation, generalizing previous results for just phase measurements with the MZI^{13,16}.

RESULTS

Phase metrology with a single-mode nonclassical state

We consider first the special case of phase sensing with a single-mode nonclassical state. This allows us to illustrate the method using the simplest nontrivial case. We generalize this method both to arbitrary single-mode transformations and multi-mode nonclassical input states in the next subsection.

In Fig. 1 we depict a general scheme for distributed quantum metrology of m phase shifts, $\theta_j, j=0, \dots, m-1$ employing a nonclassical state $\hat{\rho}$ along with arbitrary classical resources. The mode with annihilation operator \hat{a}_0 contains the state $\hat{\rho}$ which we are free to displace by a coherent amplitude a_0 and the average number of nonclassical photons is $N_q \equiv \text{Tr}[\hat{\rho}\hat{a}_0^\dagger\hat{a}_0]$, where Tr denotes the tracing operation on the basis of the mode \hat{a}_0 . Coherent states with amplitudes a_j are supplied in $m-1$ additional modes $\hat{a}_j (j=1, 2, \dots, m-1)$ (we find that there is no utility in using more input modes than unknown parameters) so that the total average number of classical photons is $N_c \equiv \sum_{j=0}^{m-1} |a_j|^2$. The modes \hat{b}_k are related to the input modes \hat{a}_j by the unitary U so $\hat{b}_k = \sum_{j=0}^{m-1} u_{kj} \hat{a}_j$ where u_{kj} are the matrix elements of U . Phase shift θ_k is applied to mode \hat{b}_k via the transformation $\exp[-i\theta_k \hat{n}_k]$, where $\hat{n}_k \equiv \hat{b}_k^\dagger \hat{b}_k$. We will perform our analysis for the special case in which $\hat{\rho}$ is a pure state ($\hat{\rho} = |\psi\rangle\langle\psi|$). At the end of this section, we will show how the result can be generalized to nonclassical mixed states using the result by Yu employing the convex roof³².

To evaluate the precision of multi-parameter estimation, we need the elements of the QFI matrix³³ for the general scheme depicted in Fig. 1 (see Methods)

$$\mathcal{F}_{jk} = 4[\langle \hat{n}_j \hat{n}_k \rangle - \langle \hat{n}_j \rangle \langle \hat{n}_k \rangle], \quad (1)$$

where $\langle \cdot \rangle$ represents the expectation value of an operator for the state $|\psi\rangle$. The complexity of this expression for \mathcal{F}_{jk} comes from the fact that in terms of the input modes, \hat{a}_j , each of the \hat{n}_k must

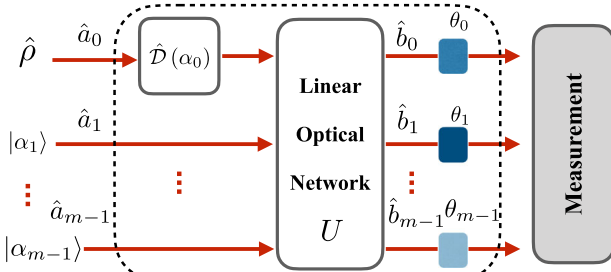


Fig. 1 A distributed quantum sensing scheme. It consists of a passive linear network with m input modes, one of which may contain a single-mode nonclassical state, $\hat{\rho}$, and it may be displaced by a coherent amplitude a_0 . The m output modes can be sent to different locations where the respective probe transformations are applied.

be replaced by $\hat{b}_k^\dagger \hat{b}_k = \sum_{j=0}^{m-1} \sum_{l=0}^{m-1} u_{lk}^* u_{kj} \hat{a}_l^\dagger \hat{a}_j$. The key to evaluating \mathcal{F}_{jk} is to employ normal ordering³⁴ of the mode operators \hat{b}_k , noting that all but one of the input modes are in coherent states. We will denote the normal ordering of a product of mode operators in the usual way by sandwiching the product between colons. Thus : $(\hat{b}_j^\dagger \hat{b}_j)^2 := \hat{b}_j^\dagger \hat{b}_j^\dagger \hat{b}_j \hat{b}_j \neq (\hat{b}_j^\dagger \hat{b}_j)^2$. Writing \mathcal{F}_{jk} in terms of normally ordered products gives

$$\mathcal{F}_{jk} = 4[\langle \hat{n}_j \hat{n}_k \rangle - \langle \hat{n}_j \rangle \langle \hat{n}_k \rangle + \delta_{jk} \langle \hat{n}_j \rangle] = : \mathcal{F}_{jk} : + \delta_{jk} 4\langle \hat{n}_j \rangle \quad (2)$$

where we have defined : \mathcal{F}_{jk} : as four times the normally ordered covariance. Since this covariance vanishes for all classical states, and since $\langle \hat{n}_j \rangle$ (the energy of mode j), is effectively independent of $|\psi\rangle$ (recall that $N_q \ll N_c$), it is : \mathcal{F}_{jk} : that is the nonclassical contribution to \mathcal{F}_{jk} . According to Eqs. (49), (50) in the section of Methods, the quantum enhancement in metrology is defined as the difference between the square precision with and without the nonclassical state:

$$\Delta\mathcal{P}_{|\psi\rangle}^2 \leq \frac{\mathbf{w}^t : \mathcal{F} : \mathbf{w}}{\|\mathbf{w}\|^4} = \frac{1}{\|\mathbf{w}\|^4} \sum_{jk} w_j w_k : \mathcal{F}_{jk} :, \quad (3)$$

where $\mathbf{w} = (w_0, \dots, w_{m-1})^t$ are the weights in distributed phase sensing²⁴ with $\sum_j w_j = 1$ and $\|\cdot\|$ is the 2-norm defined by $\|\mathbf{w}\| \equiv \sqrt{\mathbf{w}^t \mathbf{w}} = \sqrt{\sum_j w_j^2}$.

We note next that since \hat{b}_k are normally ordered, so are \hat{a}_j when we make the replacement $\hat{b}_k \rightarrow \sum_j u_{kj} \hat{a}_j$. As a result, for $j \geq 1$ we can replace \hat{a}_j with the coherent state amplitude a_j because the respective modes are in coherent states. Including the displacement of mode \hat{a}_0 , the resulting replacement is

$$\hat{b}_k \rightarrow u_{k0} \hat{a}_0 + \sum_{j=0}^{m-1} u_{kj} a_j = u_{k0} \hat{a}_0 + f_k \quad (4)$$

where we have defined the complex amplitudes $f_k \equiv \sum_{j=0}^{m-1} u_{kj} a_j$.

In the limit that $|\langle a_0^n \rangle|$ and $|\langle (a_0 a_0^\dagger)^n \rangle|$ are very much smaller than $|f_k|^n$ and $|f_k|^{2n}$ since $|f_k| \propto \sqrt{N_c} \gg \sqrt{N_q}$, we obtain according to Supplemental Methods

$$: \mathcal{F}_{jk} : = 8|u_{k0} f_k| |u_{j0} f_j| : C(\hat{X}_{\phi_k}, \hat{X}_{\phi_j}) :, \quad (5)$$

where $\phi_k = \arg[u_{k0}^* f_k]$ and $C(\hat{A}, \hat{B}) \equiv \langle \hat{A} \hat{B} \rangle - \langle \hat{A} \rangle \langle \hat{B} \rangle$ is the covariance of two operators \hat{A} and \hat{B} . Putting the expression for : \mathcal{F}_{jk} : into Eq. (3) we can now factor the double summation to write the metrological advantage in terms of a single variance:

$$\Delta\mathcal{P}_{|\psi\rangle}^2(N_c, \hat{\mathbf{n}}, \mathbf{w}) \leq \frac{8|z|^2}{\|\mathbf{w}\|^4} : V_{|\psi\rangle}(\hat{X}_\phi) :, \quad (6)$$

where $V_{|\psi\rangle}(\hat{X}_\phi) \equiv C(\hat{X}_\phi, \hat{X}_\phi)$ and we have used the arguments $\hat{\mathbf{n}} = (\hat{n}_1, \dots, \hat{n}_m)$ and \mathbf{w} in $\Delta\mathcal{P}_{|\psi\rangle}^2$ to denote distributed phase sensing²⁴, and N_c is the total amount of classical resources. Here $\phi = \arg z$ and

$$z = \sum_k w_k u_{k0} f_k^*. \quad (7)$$

So to obtain the metrological power we need to maximize $|z|^2$ in Eq. (6) over all weights $\{w_j\}$, unitary transformations U , and amplitudes of the classical inputs $\{a_j\}$. In the Supplementary Methods, we show that

$$|z|^2 \leq N_c \|\mathbf{w}\|^4. \quad (8)$$

Inserting this tight bound into the definition of the metrological power in (52), we obtain that for distributed phase measurement is:

$$\mathcal{M}_{|\psi\rangle}(N_c, \hat{\mathbf{n}}) = 8N_c \max_{\phi} : V_{|\psi\rangle}(\hat{X}_\phi) : = 2N_c \mathcal{M}_{|\psi\rangle}^F, \quad (9)$$

where $\mathcal{M}_{|\psi\rangle}^F$ is the metrological power of $|\psi\rangle$ for quadrature-displacement (force) sensing given in Eq. (54). This is one of the main results of this work that the metrological power of displacement sensing and that of phase sensing using single-mode nonclassical state are unified.

The maximum precision is given by adding the classical contribution to the quantum contribution, Eq. (9). The classical contribution is the precision obtained when all the inputs are in coherent states. In this case the QFI is diagonal where the diagonal elements are simply four times the average number of photons in the respective modes: $\mathcal{F}_{jj} = 4\langle \hat{n}_j \rangle = 4|a_j|^2$. As a result, according to Eq. (49), the square precision becomes

$$\mathcal{P}_c^2(N_c, \hat{\mathbf{n}}, \mathbf{w}) = \frac{1}{\mathbf{w}^T \mathcal{F}^{-1}(\hat{\sigma}, \hat{\mathbf{G}}) \mathbf{w}} = 4 \left[\sum_j \frac{w_j^2}{|a_j|^2} \right]^{-1}, \quad (10)$$

We can minimize the summation in the square brackets by using the Cauchy-Schwarz inequality, $(\sum_j u_j v_j)^2 \leq \sum_j u_j^2 \sum_k v_k^2$, setting $u_j = |w_j|/|a_j|$ and $v_j = |a_j|$. The result is

$$\mathcal{P}_c^2(N_c, \hat{\mathbf{n}}, \mathbf{w}) \leq 4N_c, \quad (11)$$

where the maximum is obtained (the inequality saturated) with the choice $|a_j|^2 = w_j N_c$. Both the classical and nonclassical contributions in the maximum precision can be achieved simultaneously. Since for any quadrature \hat{X}_ϕ

$$V_{|\psi\rangle}(\hat{X}_\phi) = :V_{|\psi\rangle}(\hat{X}_\phi): + \frac{1}{2}, \quad (12)$$

the maximum achievable precision for phase measurement (after maximizing the passive linear network (PLN) and the weights) is thus

$$\mathcal{P}_{|\psi\rangle}(N_c, \hat{\mathbf{n}}) = \sqrt{\mathcal{M}_{|\psi\rangle}(N_c, \hat{\mathbf{n}}) + \mathcal{P}_c^2(N_c, \hat{\mathbf{n}})} = \sqrt{8N_c \max_\phi V_{|\psi\rangle}(\hat{X}_\phi)}, \quad (13)$$

where the dependence on \mathbf{w} is dropped after the optimization procedure. This maximum precision is an amplification of the classical precision whenever $\max_\phi V_{|\psi\rangle}(\hat{X}_\phi) > 1/2$. The amplification factor is

$$\mathcal{A} = \sqrt{2 \max_\phi V_{|\psi\rangle}(\hat{X}_\phi)}. \quad (14)$$

In Supplemental Note 1, we derive explicit solutions (networks) that saturate the inequality in Eq. (8) and thus achieve the maximal precision. For the metrology of a single parameter, the maximal precision is obtained simply by displacing the nonclassical mode by the available classical energy. For two-parameter distributed quantum metrology, the maximum precision can be obtained using the balanced Mach-Zehnder interferometer. In this case

$$U = \frac{1}{\sqrt{2}} \begin{pmatrix} 1 & e^{i\beta} \\ -e^{-i\beta} & 1 \end{pmatrix} \quad (15)$$

where β is the phase shift of the MZI beam-splitter. For the maximum precision, one chooses the weightings $w_1 = -w_2 = 1/2$.

Metrology of any single-mode transformation with multi-mode nonclassical states

We now extend the results obtained in the previous section in two ways. We extend the microscopic nonclassical input to all pure multi-mode states, and we extend the phase shift to all single-mode transformations for which the metrological power is well-defined (see Fig. 2). To this end, we consider an arbitrary Hermitian single-mode transformation \hat{G} expressed as a normally ordered

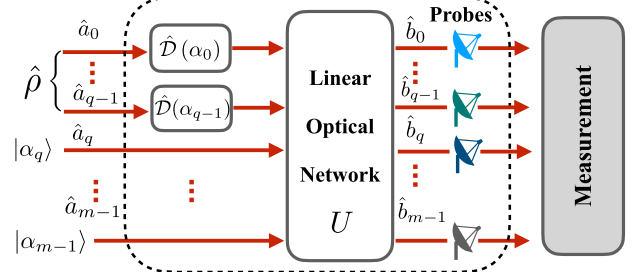


Fig. 2 Distributed quantum metrology with a multi-mode nonclassical input state. It is a generalization to Fig. 1 by considering a multi-mode nonclassical input state $\hat{\rho}$. The multi-mode nonclassical state is displaced by a multi-mode coherent state $|a_0\rangle \otimes \dots \otimes |a_{q-1}\rangle$. Also, the probes are more general than the standard phase shifts, which are given by nonlinear operators in Eq. (17).

power series of the annihilation and creation operators:

$$\hat{G} = \sum_{q=0}^p \sum_{j=0}^q \kappa_{qj} \hat{b}^{\dagger(q-j)} \hat{b}^j, \quad (16)$$

where κ_{qj} are the coefficients to ensure \hat{G} Hermitian. In this power series the number of mode operators in each term (the order of each term) is given by q . We will find that every term of order q contributes to the metrological power a term proportional to N_c^{q-1} . This has two consequences. First, since the metrological power is defined in the limit of large N_c , it is undefined if the power series is infinite. We, therefore, restrict \hat{G} to transformations for which the maximum value of q is $p < \infty$. Second, in the limit of large N_c it is only those terms of order p that contribute. So for the purposes of calculating the metrological power we need only retain those terms and can thus write \hat{G} as

$$\hat{G} = \sum_{j=0}^p \kappa_j \hat{b}^{\dagger(p-j)} \hat{b}^j. \quad (17)$$

Because \hat{G} is Hermitian $\kappa_j = \kappa_{p-j}^*$, and we normalize \hat{G} by setting $\sum \kappa_j = 1$. Substituting \hat{G} in Eq. (43), the matrix elements of the QFI for a pure state are given by

$$\mathcal{F}_{uv} = 4[\langle \hat{G}_u \hat{G}_v \rangle - \langle \hat{G}_u \rangle \langle \hat{G}_v \rangle] = 4 \sum_{j,k} \kappa_j \kappa_k [\langle \hat{C}_j^{(u)} \hat{C}_k^{(v)} \rangle - \langle \hat{C}_j^{(u)} \rangle \langle \hat{C}_k^{(v)} \rangle], \quad (18)$$

where $\hat{G}_u = \sum_{j=0}^p \kappa_j \hat{b}_u^{\dagger(p-j)} \hat{b}_u^j$ and we have defined $\hat{C}_k^{(v)} = \hat{b}_v^{\dagger(p-k)} \hat{b}_v^k$. To split the QFI into the classical and quantum contributions we need to calculate $\langle : \hat{C}_j^{(u)} \hat{C}_k^{(v)} : \rangle$. Deriving the identity

$$\hat{b}^k \hat{b}^{\dagger n} = \hat{b}^{\dagger n} \hat{b}^k + \sum_{j=1}^{\min(k,n)} \frac{k!n!}{(k-j)!(n-j)!j!} \hat{b}^{\dagger n-j} \hat{b}^{k-j}, \quad (19)$$

and noting that only the terms with at least $p-2$ mode operators will contribute in the limit of large N_c we obtain according to Supplemental Methods

$$\begin{aligned} \mathcal{F}_{uv} &= : \mathcal{F}_{uv} : + 4\delta_{uv} \sum_{jk} \kappa_j \kappa_k (p-k)j \langle \hat{b}_u^{\dagger(2p-j-k-1)} \hat{b}_u^{j+k-1} \rangle \\ &= : \mathcal{F}_{uv} : + 4\delta_{uv} |f_u|^{2p-2} \left| \sum_{k=1}^{p-1} \kappa_k k e^{2iky_u} \right|^2, \end{aligned} \quad (20)$$

where we have defined the phases $y_u = \arg(f_u)$.

The classical contribution to the QFI matrix is the second term in Eq. (20), namely

$$\mathcal{F}_{uv}^{(c)} \equiv 4\delta_{uv} |f_u|^{2p-2} \left| \sum_{k=1}^{p-1} \kappa_k k e^{2iky_u} \right|^2. \quad (21)$$

We now recall that to maximize the precision, the QFI matrix must be such as to have \mathbf{w} as an eigenvector²⁴. Since we see from Eq. (21) that the classical contribution to this matrix, \mathcal{F}_{uv} , is diagonal, this can only be satisfied if \mathcal{F} is proportional to the identity or \mathbf{w} has only one non-zero element. In fact, the latter is merely the special case of the former in which $m = 1$. We also note that the final summation in Eq. (20) is maximized by choosing the appropriate value for the phases γ_u . Since these phases can be chosen arbitrarily and independently of $|f_u|$, the classical contribution to the QFI matrix is

$$\mathcal{F}_{uv}^{(c)} = 4\delta_{uv}B(\kappa)|f_u|^{2(p-1)} = 4\delta_{uv}B(\kappa)\frac{N_c^{p-1}}{m^{p-1}}, \quad (22)$$

where

$$B(\kappa) \equiv \max_y \left| \sum_{k=1}^{p-1} \kappa_k k e^{2iky} \right|^2. \quad (23)$$

To obtain the RHS of Eq. (22), we have chosen all the $|f_u|$ to be equal ($|f_u|^2 = N_c/m$) so that \mathcal{F}_{uv} is proportional to the identity. As per Eq. (49) the upper bound on the square precision is now

$$\mathcal{P}_c^2(N_c, \hat{\mathbf{G}}, \mathbf{w}) \leq 4B(\kappa)\frac{N_c^{p-1}}{m^{p-1}} \frac{1}{\|\mathbf{w}\|^2} \leq 4B(\kappa)\frac{N_c^{p-1}}{m^{p-2}} \leq 4B(\kappa)N_c^{p-1}, \quad (24)$$

we have used the arguments $\hat{\mathbf{G}} = (\hat{G}_1, \dots, \hat{G}_m)$ and \mathbf{w} in \mathcal{P}_c^2 to denote the general distributed sensing with an arbitrary single-mode Hermitian transformation. Here the second inequality is maximized by choosing \mathbf{w} to be equally distributed over the m parameters. Note that when $p=2$ (phase measurement) the maximum precision is the same for any number of parameters, i.e., independent of m . However, when the transformation \hat{G} is nonlinear ($p \geq 3$) the precision reduces as the number of parameters is increased. Thus the maximum classical precision is obtained for $m=1$ as given in the last inequality in the above equation.

We now turn to calculating the quantum contribution to the QFI, namely : \mathcal{F}_{uv} :. Instead of a single input mode containing a nonclassical state, now input modes with mode operators a_0, a_1, \dots, a_{q-1} contain a joint nonclassical state (Fig. 2). As a result the transformation in Eq. (4) is replaced by

$$\hat{b}_u \rightarrow \sum_{l=0}^{q-1} u_{ul} \hat{a}_l + f_u \quad (25)$$

and as before $f_u = \sum_{l=0}^{m-1} u_{ul} a_l$. We rewrite this sum over the nonclassical modes a_l as a single-mode operator:

$$\hat{b}_u \rightarrow g_u \hat{d}_u + f_u \quad (26)$$

where $\hat{d}_u = \frac{1}{g_u} \sum_{l=0}^{q-1} u_{ul} \hat{a}_l$ and $g_u = \left(\sum_{l=0}^{q-1} |u_{ul}|^2 \right)^{1/2}$. Making the above replacement in : \mathcal{F}_{uv} : and keeping only those terms with no more than two factors of \hat{d}_u as in the previous section, we find that we can write it in the form according to Supplemental Methods

$$\lim_{N_c \rightarrow \infty} : \mathcal{F}_{uv} : = 4(\langle : \hat{A}_u \hat{A}_v : \rangle - \langle \hat{A}_u \rangle \langle \hat{A}_v \rangle), \quad (27)$$

where $\hat{A}_u = \sum_{j=0}^p \kappa_j f_u^{*p-j-1} f_u^{j-1} g_u \left((p-j) f_u \hat{d}_u + j f_u^* \hat{d}_u \right)$. By substituting : \mathcal{F}_{uv} : in Eq. (3), we obtain

$$\Delta \mathcal{P}_{|\psi\rangle}^2(N_c, \hat{\mathbf{G}}, \mathbf{w}) \leq \max_{\text{PLN}, \mathbf{w}} \frac{8|z|^2}{\|\mathbf{w}\|^4} : V_{|\psi\rangle}(\hat{X}_d) :, \quad (28)$$

Here $|z|^2 = B(\kappa) \sum_{l=0}^{q-1} |c_l|^2$ and $\hat{X}_d = (\hat{d} + \hat{d}^\dagger)/\sqrt{2}$, where the mode operator \hat{d} is the linear combination of nonclassical input modes

$$\hat{d} = \frac{\sum_{l=0}^{q-1} c_l \hat{a}_l}{\sqrt{\sum_{l=0}^{q-1} |c_l|^2}} \quad (29)$$

with coefficients $c_l = \sum_u w_{ul} |f_u|^{p-1} u_{ul} = \mathbf{v} \cdot \mathbf{u}_l$. Here the elements of the vector \mathbf{v} are $v_u = w_u |f_u|^{p-1}$. We need to choose \hat{d} so that it is the linear combination of the nonclassical input modes that has the maximum quadrature variance, and also maximize the sum $\sum_{l=0}^{q-1} |c_l|^2$. To this end, we first note that the set of q vectors \mathbf{u}_l are orthonormal ($q \leq m$) and can be chosen arbitrarily. We choose them so that the vector \mathbf{v} lies in the q -dimensional space that they span. This automatically ensures that

$$\sum_{l=0}^{q-1} |c_l|^2 = \|\mathbf{v}\|^2. \quad (30)$$

which is its maximum value. Since the vectors \mathbf{u}_l are a basis for a q -dimensional space containing \mathbf{v} , we can choose the coefficients c_l arbitrarily merely by rotating this basis. In particular we can choose c_l so that \hat{d} gives the maximum quadrature variance.

We now use the fact that $\|\mathbf{v}\|^2 = (\mathbf{v} \cdot \mathbf{r})^2$ when \mathbf{r} is a unit vector aligned with \mathbf{v} . This allows us to write

$$|z|^2 = B(\kappa) \|\mathbf{v}\|^2 = B(\kappa) \left(\sum_{u=0}^{m-1} w_u |f_u|^{(p-1)} r_u \right)^2. \quad (31)$$

Apart from the fact that f_u is raised to a higher power, the summation in $|z|^2$ has exactly the same form as that in Eq. (7) for phase sensing with a single-mode nonclassical state. We, therefore, use the same procedure to optimize it and obtain (see Supplemental Methods)

$$|z|^2 \leq N_c^{p-1} B(\kappa) \|\mathbf{w}\|^4. \quad (32)$$

This time, however, the upper bound can only be saturated when the vector $(f_0, f_1, \dots, f_{m-1})^T$ has only one non-zero element. Since $\sum_u |f_u|^2 = N_c$ we have $\sum_u |f_u|^{2(p-1)} \leq N_c^{p-1}$ where for $p \geq 3$ the equality holds only if the vector has only one non-zero element. In this case, to optimize the precision, \mathbf{w} must also have only one non-zero element (single-parameter metrology). Thus for a fixed available classical energy, for nonlinear metrology ($p \geq 3$) the precision decreases as the number of measured parameters is increased. This is not the case for linear metrology (phase measurement).

Substituting Eq. (32) into Eq. (28), we obtain the maximum nonclassical contribution to the square precision, which is also the metrological power:

$$\mathcal{M}_{|\psi\rangle}(N_c, \hat{\mathbf{G}}) = \max_{\text{PLN}, \mathbf{w}} \Delta \mathcal{P}_{|\psi\rangle}^2(N_c, \hat{\mathbf{G}}, \mathbf{w}) = 8N_c^{p-1} B(\kappa) \max_d : V_{|\psi\rangle}(\hat{X}_d) :, \quad (33)$$

where the maximization over d is over all passive linear transformations of the nonclassical input modes. Adding together the classical and nonclassical contributions to the precision, Eqs. (24) and (33), gives us the maximum precision obtainable with nonlinear metrology, strong coherent states with total photon number N_c , and weak nonclassical states:

$$\mathcal{P}_{|\psi\rangle}(N_c, \hat{\mathbf{G}}) = \sqrt{8N_c^{p-1} B(\kappa) \max_d V_{|\psi\rangle}(\hat{X}_d)}. \quad (34)$$

The expression for the maximum precision, Eq. (34), shows that for a multi-mode input this precision is the same as for a single-mode input when the single mode has the same maximum quadrature variance as the optimal linear combination of the multiple nonclassical input modes. This shows us immediately that the following two-stage linear network will achieve maximal precision. First, we construct a network that takes the multi-mode nonclassical state as an input and produces the linear combination of the input modes that has the maximal quadrature variance at one of its outputs. Second, we feed this output into a network in the scheme that achieves the maximum

precision for a single-mode nonclassical input. We show in Supplemental Note 1 that the MZI is one such network.

Metrological power for mixed states

So far we have calculated the metrological power only for pure states. We can now use Yu's theorem^{32,35}, given in Eq. (39), to extend our results to all mixed states. Yu's theorem is only valid for single-parameter metrology, but since the maximum nonclassical contribution to the square precision (the metrological power) can be achieved for $m = 1$, Yu's theorem is sufficient for our purposes. We have

$$\begin{aligned}\mathcal{F}(\hat{\rho}, \hat{G}) &= \min_{\{p_n, |\psi_n\rangle\}} \sum_n p_n \mathcal{F}(|\psi_n\rangle\langle\psi_n|, \hat{G}) \\ &= 8N_c^{p-1} B(\kappa) \max_d \left[\min_{\{p_n, |\psi_n\rangle\}} \sum_n p_n V_{|\psi_n\rangle}(\hat{X}_d) \right] \\ &= 8N_c^{p-1} B(\kappa) \max_d \mathcal{F}(\hat{\rho}, \hat{X}_d)\end{aligned}\quad (35)$$

where the second line is obtained by using the fact that for single-parameter metrology the QFI is the square precision which for pure states is in turn given by Eq.(34). We recall that $B(\kappa)$ is defined in Eq.(23), and the parameters κ_j define the transformation \hat{G} , given in Eq.(17). Here $\mathcal{F}(\hat{\rho}, \hat{X}_d)$ is the QFI for quadrature-displacement of the operator $\hat{X}_d = (\hat{d} + \hat{d}^\dagger)/\sqrt{2}$. The maximization is over a mode \hat{d} that is a passive linear transformation of the nonclassical input modes. Note that there is only a single maximization over the mode \hat{d} because when using the mixed state for metrology we can only use one linear network (we cannot use a different linear network for each state in the decomposition of $\hat{\rho}$). We note that there is a closed-form expression for the QFI, which can be used to calculate $\mathcal{F}(\hat{\rho}, \hat{X}_d)$ for a given $\hat{\rho}$ and \hat{X}_d ³⁶.

Performing the analysis in Eq.(35), but splitting the QFI into its quantum and classical parts, we have the equivalent result for the metrological power for a mixed state

$$\mathcal{M}_p(N_c, \hat{G}) = 8N_c^{p-1} B(\kappa) \max_d \left[\min_{\{p_n, |\psi_n\rangle\}} \sum_n p_n : V_{|\psi_n\rangle}(\hat{X}_d) : \right] = 4N_c^{p-1} B(\kappa) \mathcal{M}_p^F. \quad (36)$$

A practical example: LIGO

Adding a microscopic nonclassical state to a measurement scheme that employs macroscopic laser light can greatly reduce the laser power required to achieve a given measurement precision. There are two quite distinct situations in which this is useful. The first is

whenever we wish to reduce the overall power consumption of a measuring device. The second is when there is a limit to the amount of laser power that can be applied to the object being measured.

Microscopic nonclassical states are useful in reducing overall power consumption only if they can be produced without using more power than they save. Since experimental technology has not yet reached the point at which nonclassical states can be produced with the necessary efficiency, applications of these states are presently restricted to measurements in which there is a practical limitation to laser power. This can be true for measurements on various biological systems that are fragile under heating, and it is true for LIGO (the laser-interferometric gravitational observatory) in which one needs to obtain the maximum possible precision.

The use of squeezed states in improving the precision of LIGO^{6,37} provides an example to connect our results directly to an application. LIGO is an interferometer designed to measure extremely small changes in distance induced by gravity waves⁶. A change in distance between the two end mirrors of an optical cavity translates to a phase shift of the light that is output from the cavity. An interferometer measures the phase difference between two phase shifts, each applied respectively to two modes that are referred to as the 'arms' of the interferometer. This is the configuration referred to in our treatment above as distributed metrology of two-phase shifts. For the LIGO interferometer there are two cavities, one inserted into each arm, that apply the respective phase shifts. The LIGO interferometer is in the Michelson configuration as opposed to the Mach-Zehnder configuration that we use in our analysis, but the two are equivalent and are shown together in Fig. 3. The only difference between these configurations is that the Mach-Zehnder uses two beam-splitters (A and B) whereas the Michelson uses a single beam-splitter twice: it uses the same beam-slit (C) to split the input and to combine the two arms to produce the output.

Here we have shown that the method originally suggested by Caves in 1981² and now being used by LIGO³⁸ is in fact the optimal way to measure a phase difference using a weak nonclassical state. The LIGO configuration is a distributed phase measurement of two-phase shifts in which one input mode is a strong coherent state and the other is a weak squeezed state. The precision of this configuration is given in Eq. (13). In implementing this scheme using continuous-wave inputs the variance of the measurement error reduces as the inverse of the measurement time; the longer we measure the output of the interferometer the more photons we detect and the more accurate the measurement. The total number of photons used for the measurement is the total number of photons detected in the measurement time t

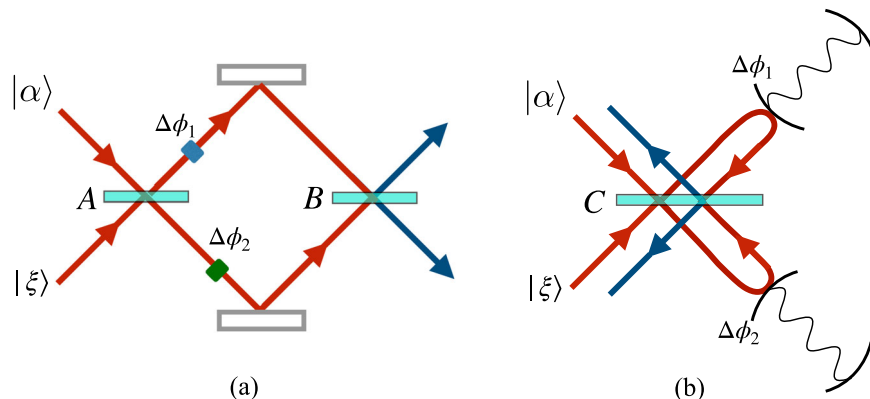


Fig. 3 The equivalence between the Mach-Zehnder interferometer. a that we use in our analysis and the Michelson interferometer **b** used by LIGO. While the Mach-Zehnder uses one beam-splitter (A) at the input and a second (B) for the output, the Michelson uses the same beam-splitter (C) twice: first to combine the inputs and second to produce the output. In the LIGO interferometer the phase shifts $\Delta\phi_1$ and $\Delta\phi_2$ are applied by two optical cavities.

being $N_c = Pt/(\hbar\omega_0)$ where P is the laser power for the coherent input and ω_0 is the frequency of the light. The variance of the measurement error thus reduces with time as C/t where, for classical inputs, the constant is $C = \hbar\omega_0/(4P)$. If the time t is measured in seconds then the square root of this constant is referred to as the phase error 'per $\sqrt{\text{Hz}}$ '. For a nonclassical input, as per Eq. (13), the phase error per $\sqrt{\text{Hz}}$ is

$$\Delta\phi = \left(\frac{8P}{\hbar\omega_0} \max_{\phi} V_{|\psi\rangle}(\hat{X}_\phi) \right)^{-1/2} = \sqrt{\frac{\hbar\omega_0}{4P}} e^{-r}, \quad (37)$$

where r is the 'squeezing parameter' that characterizes the amount by which the nonclassical input is squeezed³⁹. This maximum possible precision will be degraded by imperfections such as loss in the interferometer which reduces the squeezing and loss at the photo-detectors.

For LIGO there is an additional source of error that is quite separate from the noise that limits the maximum precision for phase metrology^{2,38}. Changes in the distance between the cavity mirrors change the phase of the cavity output. The quantum fluctuations in the laser intensity impart momentum and therefore position noise to the mirrors, and these position fluctuations produce phase noise^{40,41}. This noise is the quantum 'back-action' of the position measurement⁴². Squeezing the input light increases the fundamental precision of the measurement but also increases the phase noise power from the back-action by the factor e^{2r} . At the operating laser power for LIGO, $P = 200$ kW, measuring a signal at 400 Hz without squeezed light the back-action phase noise power per unit frequency is $\sim 10^{-27} \text{ rad}^2 \text{ Hz}^{-1}$ (see Supplemental Note 2). Since the measurement error for LIGO at this power is $\sim 10^{-25} \text{ rad}^2 \text{ Hz}^{-1}$ will increase the accuracy up to a squeezing factor of $e^{2r} \approx 10$ before the back-action phase noise would prevent further increases. The squeezing factor of the squeezed states presently injected into the LIGO L1 interferometer is 7.2 dB or $e^{2r} = 5.2$ ³⁸. If there were no losses this would reduce the error of the phase measurement by a factor of $e^{-r} = 1/2.3$. Losses reduce the squeezing to 2.7 dB which results in a more modest error reduction of 36%. This example makes clear the difficulty of using nonclassical states for metrology: one must not only reduce all classical sources of noise so that they are much smaller than the very tiny fundamental quantum noise, as well as creating a nonclassical state, but protect this state from loss long enough to make use of it. All of these elements have been achieved by LIGO. Improvements are also planned that will allow squeezing to increase the precision further.

DISCUSSION

Weak nonclassical light is able to amplify the precision of measurements that employ much stronger coherent light. Here we have determined the maximum amplification that can be achieved in this way by every quantum state of light (more generally, any bosonic field), for local and distributed quantum metrology that employs any single-mode transformation. We have shown that for the measurement of all single-mode quantities the maximum amplification depends on the same quantity, being the QFI for displacement metrology. For single-mode pure states this QFI is simply the maximum quadrature variance. Our analysis also reveals the linear networks that can be used to achieve maximum precision.

The method we have used to obtain our results should also enable answering the same question for multi-mode transformations, which constitutes an interesting question for future work. We also expect that our results will have applications to the resource theory of nonclassicality, something that we have not explored here.

METHODS

Local and distributed quantum metrology

Quantum metrology refers to the measurement of a classical quantity or quantities using a quantum system as a probe. First consider metrology of a single quantity, ξ . For a quantum system to act as a probe its state must be affected in some way by ξ so that information about ξ can be extracted by making a measurement on the system. We can write the effect of ξ on the system as the action of an operator $U_\xi = e^{-i\xi\hat{G}}$ where \hat{G} (the 'metrological transformation') is a Hermitian operator¹. As an example, if we are measuring the size of a force then $\hat{G} = \hat{b}e^{-i\phi}/\sqrt{2} + \text{H.c.} \equiv \hat{X}_\phi$ is the position operator, where \hat{b} is the mode operator at the probe and ϕ is the quadrature phase. If we are measuring a phase shift induced in a mode by a distance or a duration, then $\hat{G} = \hat{b}^\dagger \hat{b}$. The amount of information that can be obtained about ξ by measuring the system depends on the state in which the system is prepared prior to the action of $U(\xi)$. If we denote this state by $\hat{\sigma}$, then the maximum information that can be obtained about ξ (the 'sensitivity' of the probe) is captured by the QFI, denoted by $\mathcal{F}(\hat{\sigma}, \hat{G})$. For a pure state $\hat{\sigma} = |\psi\rangle\langle\psi|$, the QFI reduces to four times the variance of \hat{G} ³³, namely

$$\mathcal{F}(|\psi_n\rangle\langle\psi_n|, \hat{G}) \equiv 4V_{|\psi\rangle}(\hat{G}) = 4\left(\langle\hat{G}^2\rangle - \langle\hat{G}\rangle^2\right), \quad (38)$$

where $\langle\hat{A}\rangle \equiv \langle\psi|\hat{A}|\psi\rangle$ for any operator \hat{A} . For mixed states, Yu's theorem states that the QFI can be written in terms of that for pure states as^{32,35}

$$\mathcal{F}(\hat{\sigma}, \hat{G}) = \min_{\{p_n, |\psi_n\rangle\}} \sum_n p_n \mathcal{F}(|\psi_n\rangle\langle\psi_n|, \hat{G}), \quad (39)$$

where the minimization is over all ensembles that decompose $\hat{\sigma}$ (all ensembles $\{p_n, |\psi_n\rangle\}$ for which $\hat{\sigma} = \sum_n p_n |\psi_n\rangle\langle\psi_n|$ and $p_n > 0, \forall n$). The expression on the RHS of Eq. (39) is referred to as the convex roof of \mathcal{F} .

The QFI quantifies the minimum error with which the parameter ξ can be obtained, $\Delta\xi$, by measuring the probe system given the initial state $\hat{\sigma}$ and transformation \hat{G} via the relation^{36,43}

$$\Delta\xi \geq \frac{1}{\sqrt{M\mathcal{F}(\hat{\sigma}, \hat{G})}} \quad (40)$$

where M is the (sufficiently large) number of repetitions of the metrology procedure. This relationship is referred to as the quantum Cramér-Rao bound^{36,43}.

Defining the precision of a metrology protocol, $\mathcal{P}(\hat{\sigma}, \hat{G})$, as the inverse of the minimum error per root repetition, we have

$$\mathcal{P}(\hat{\sigma}, \hat{G}) \equiv \sqrt{\mathcal{F}(\hat{\sigma}, \hat{G})}. \quad (41)$$

Distributed quantum metrology is a straightforward generalization of the metrology process considered above in which a quantum system is used to measure a function of a set of m parameters $\{\xi_j\}$ ^{22–25,44}. Usually, these parameters are considered to be values of the same physical quantity at different locations. Here we will restrict ourselves to determining (estimating) a linear combination of the parameters. Our analysis is also applicable to the simultaneous estimation of all the parameters⁴⁵.

In Fig. 1, we display a distributed quantum sensing scheme with an initial input state $\hat{\sigma} = \mathcal{D}(a_0)\hat{p}\mathcal{D}^\dagger(a_0) \otimes |a_1\rangle\langle a_1| \cdots \otimes |a_{m-1}\rangle\langle a_{m-1}|$, in which one of the input modes contains an arbitrary quantum state, \hat{p} , displaced by a coherent displacement $\mathcal{D}(a_0) \equiv \exp(a_0 a_0^\dagger - a_0^* a_0)$ and the rest are in coherent states, $|a_j\rangle$ ($j = 1, 2, \dots, m-1$). After combining all the input modes with an arbitrary PLN each transformation is applied to a different mode. This allows each mode to be sent to a different location where the respective transformations are applied. Distributed quantum metrology is not the most general way to implement a

measurement of a global parameter. In Supplemental Note 3, we depict the most general linear scheme for this purpose. We show that in the regime in which we are interested here, that is when the classical input energy is much larger than that of the nonclassical states, the most general scheme can improve upon the precision of distributed quantum metrology only by the factor m , the origin of which is a trivial classical effect resulting from applying all the phase shifts in sequence to a single mode.

As per Fig. 1, defining mode operators $\hat{b}_j, j = 0, \dots, m-1$ for each of m modes at the probe, and operators $\hat{G}_j = f(\hat{b}_j, \hat{b}_j^\dagger)$ in which f is some function, the action of the set of parameters on the probe system is given by the product

$$U_\xi = \prod_j \exp[-i\xi_j \hat{G}_j]. \quad (42)$$

If the input state $\hat{\rho}$ is a pure state then the QFI for this multi-parameter estimation problem, which we again denote by \mathcal{F} , is now a matrix whose elements are^{33,43}

$$\mathcal{F}_{jk} = 4(\langle \hat{G}_j \hat{G}_k \rangle - \langle \hat{G}_j \rangle \langle \hat{G}_k \rangle). \quad (43)$$

For simultaneous estimation of all the parameters ξ_j with a set of unbiased estimators Ξ_j , the error of the estimators is now given by a covariance matrix, $\text{cov}(\Xi)$, whose matrix elements are

$$\text{cov}(\Xi)_{jk} = \langle (\Xi_j - \xi_j)(\Xi_k - \xi_k) \rangle, \quad (44)$$

where $\langle O \rangle$ is the average value of the quantity O . Note that here the average is not only a quantum expectation over the joint multi-mode state input to the PLN but also over the possible values of the parameters and the results of the measurement for each repetition of the metrology scheme. The multi-parameter version of the quantum Cramér-Rao bound^{33,43} is

$$\text{cov}(\Xi) \geq (M\mathcal{F})^{-1}, \quad (45)$$

where M is again the number of independent repetitions of the metrology process.

For estimating a linear combination of the parameters, namely

$$\xi = \sum_j w_j \xi_j, \quad \text{with} \quad \sum_j |w_j| = 1, \quad (46)$$

which is referred to as a global estimate^{22–25,44}, the measurement uncertainty in the estimate of ξ is²⁴

$$\Delta\xi \geq \sqrt{\frac{w^t \mathcal{F}^{-1} w}{M}} \quad (47)$$

in which we have defined the vector $w = (w_1, \dots, w_m)^t$. The above inequality is not well-suited to minimizing $\Delta\xi$, however, because it involves the inverse of the QFI matrix. We can obtain a much simpler lower bound by using the Cauchy-Schwartz inequality to show that²⁴

$$\Delta\xi \geq \sqrt{\frac{w^t \mathcal{F}^{-1} w}{M}} \geq \frac{\|w\|^2}{\sqrt{M w^t \mathcal{F} w}} \quad (48)$$

The beauty of the second inequality is that it becomes an equality when w is an eigenvector of the QFI matrix, \mathcal{F} , and the RHS of Eq. (47) is also minimized when w is an eigenvector of \mathcal{F} . We can therefore find the maximum precision by minimizing the RHS of Eq. (48) under the constraint that w is an eigenvector of \mathcal{F} .

We define the precision of a distributed quantum metrology protocol by

$$\mathcal{P}(\hat{\sigma}, \hat{\mathbf{G}}, \mathbf{w}) \equiv (w^t \mathcal{F}^{-1}(\hat{\sigma}, \hat{\mathbf{G}}) w)^{-1/2} \leq \frac{1}{\|w\|^2} \sqrt{w^t \mathcal{F}(\hat{\sigma}, \hat{\mathbf{G}}) w}, \quad (49)$$

W. Ge et al.

where $\hat{\mathbf{G}} = (\hat{G}_1, \dots, \hat{G}_m)$ denotes the set of transformations for m probes. Note that a distributed quantum metrology protocol automatically reduces to a single-parameter protocol when $m = 1$.

Metrological power

A classical metrology procedure is one in which the initial state, $\hat{\sigma}$, consists of any number of modes in coherent states $|\alpha_k\rangle$. An optimal classical metrology procedure for a given set of transformations $\{\hat{G}_j\}$ is one that achieves the maximum QFI for the total average number of photons, N_c . Obtaining an optimal protocol, by definition, involves maximizing over all PLNs as well as the choice of weightings, \mathbf{w} .

Consider an optimal classical metrology procedure \mathbb{M} , that employs m transformations $\hat{\mathbf{G}}$ to measure a single ($m = 1$) or global parameter $\xi = \sum_{j=0}^{m-1} w_j \xi_j$. Let us denote the precision of \mathbb{M} by $\mathcal{P}_c(N_c, \hat{\mathbf{G}}, \mathbf{w})$. Now define an optimal metrology protocol that employs classical states with the same total number of photons N_c and transformations $\hat{\mathbf{G}}$, but this time with an additional mode containing a nonclassical state $\hat{\rho}$ with average photon number N_q . Since N_q is required to be negligible compared to N_c , there is little point in including N_q in the resource count for the protocol. Hence, we will denote the precision of this protocol by $\mathcal{P}_{\hat{\rho}}(N_c, \hat{\mathbf{G}}, \mathbf{w})$. The increase in the square of the precision resulting from adding the nonclassical state is

$$\Delta\mathcal{P}_{\hat{\rho}}^2(N_c, \hat{\mathbf{G}}, \mathbf{w}) = \mathcal{P}_{\hat{\rho}}^2(N_c, \hat{\mathbf{G}}, \mathbf{w}) - \mathcal{P}_c^2(N_c, \hat{\mathbf{G}}, \mathbf{w}). \quad (50)$$

We wish to define the metrological power as this increase in the square precision as $N_c \rightarrow \infty$ for a fixed N_q . We use the square of the precision so that the metrological power is linear in the QFI. If $\Delta\mathcal{P}_{\hat{\rho}}^2(N_c, \hat{\mathbf{G}}, \mathbf{w})$ depends on \mathbf{w} and the PLN involving the coherent states and the unitary U , then we also maximize over \mathbf{w} and the PLN. To be precise, in our definition we have to be a little careful because the metrological power scales with the resource N_c and thus tends to infinity as $N_c \rightarrow \infty$.

Allowing the elements of $\hat{\mathbf{G}}$ to take the general form

$$\hat{G}_j = \sum_{l=0}^p \sum_{r=0}^l K_{lr} \hat{b}_j^{\dagger l-r} \hat{b}_j^r, \quad (51)$$

we will find that for large N_c this maximum increase is proportional to N_c^{p-1} . We can thus define metrological power as

$$\mathcal{M}_{\hat{\rho}}(N_c, \hat{\mathbf{G}}) = \max_{\mathbf{w}, \text{PLN}} \left[\lim_{N_c \rightarrow \infty} \frac{\Delta\mathcal{P}_{\hat{\rho}}^2(N_c, \hat{\mathbf{G}}, \mathbf{w})}{N_c^{p-1}} \right] N_c^{p-1}. \quad (52)$$

There is one transformation for which the maximum precision is straightforward to calculate and thus the metrological power is already known²¹. This transformation is a displacement in phase-space (corresponding to measuring force or acceleration), for which $\hat{G} = \hat{X}_\phi \equiv \hat{b}e^{-i\phi}/\sqrt{2} + \text{H.c.}$ This transformation is unique in that the maximum precision is achieved using the nonclassical state alone; there is no benefit to combining the nonclassical state with classical states. Thus the QFI for a displacement transformation using state $|\psi\rangle$, which we will denote by \mathcal{F}_ϕ , is given simply by four times the variance of \hat{X}_ϕ for $|\psi\rangle$. Since the quadrature angle, ϕ , can be selected merely by using a phase shift, we must maximize over it to determine the maximum precision^{46,47}. According to Eq. (41), the maximum precision in this case is

$$\mathcal{P}_{\max}^F = \sqrt{\max_\phi \mathcal{F}_\phi} = 2 \left(\max_\phi V_{|\psi\rangle}(\hat{X}_\phi) \right)^{1/2}. \quad (53)$$

The corresponding metrological power for displacement sensing is

$$\mathcal{M}_{|\psi\rangle}^F = 4 \left(\max_\phi V_{|\psi\rangle}(\hat{X}_\phi) - \frac{1}{2} \right). \quad (54)$$

The difficulty of calculating the maximum precision for all other transformations, in which \hat{G} has terms involving products of two or more mode operators, is the complexity of the expression for the QFI when considering one or more input quantum states, additional coherent inputs, and an arbitrary PLN^{20,21,24,25,48–58}. We show in the section of Results that this expression can be made tractable by a judicious application of normal ordering³⁴. It is then possible to maximize the result over all PLNs even when \hat{G} involves arbitrarily high-order nonlinearities and multiple nonclassical input modes.

DATA AVAILABILITY

No data sets were generated or analyzed during the current study.

Received: 23 June 2022; Accepted: 23 December 2022;

Published online: 11 January 2023

REFERENCES

1. Giovannetti, V., Lloyd, S. & Maccone, L. Quantum metrology. *Phys. Rev. Lett.* **96**, 010401 (2006).
2. Caves, C. M. Quantum-mechanical noise in an interferometer. *Phys. Rev. D* **23**, 1693–1708 (1981).
3. Holland, M. J. & Burnett, K. Interferometric detection of optical phase shifts at the heisenberg limit. *Phys. Rev. Lett.* **71**, 1355–1358 (1993).
4. Pezzé, L. & Smerzi, A. Mach-zehnder interferometry at the heisenberg limit with coherent and squeezed-vacuum light. *Phys. Rev. Lett.* **100**, 073601 (2008).
5. Liu, J., Jing, X. & Wang, X. Phase-matching condition for enhancement of phase sensitivity in quantum metrology. *Phys. Rev. A* **88**, 042316– (2013).
6. Aasi, J. et al. Enhanced sensitivity of the ligo gravitational wave detector by using squeezed states of light. *Nat. Photonics* **7**, 613 EP – (2013).
7. Wollman, E. E. et al. Quantum squeezing of motion in a mechanical resonator. *Science* **349**, 952–955 (2015).
8. Burd, S. C. et al. Quantum amplification of mechanical oscillator motion. *Science* **364**, 1163–1165 (2019).
9. Taylor, M. A. & Bowen, W. P. Quantum metrology and its application in biology. *Phys. Rep.* **615**, 1–59 (2016).
10. Yu, J. et al. Quantum enhanced optical phase estimation with a squeezed thermal state. *Phys. Rev. Appl.* **13**, 024037 (2020).
11. McCuller, L. et al. Frequency-dependent squeezing for advanced ligo. *Phys. Rev. Lett.* **124**, 171102 (2020).
12. Zhao, Y. et al. Frequency-dependent squeezed vacuum source for broadband quantum noise reduction in advanced gravitational-wave detectors. *Phys. Rev. Lett.* **124**, 171101 (2020).
13. Lang, M. D. & Caves, C. M. Optimal quantum-enhanced interferometry using a laser power source. *Phys. Rev. Lett.* **111**, 173601 (2013).
14. Huang, C.-C. Optical heterodyne profilometer. *Opt. Eng.* **23**, 365 (1984).
15. Demkowicz-Dobrzański, R., Jarzyna, M., Kołodyński, J. & Wolf, E. *Chapter Four - Quantum Limits in Optical Interferometry*, vol. 60, 345–435 (Elsevier, 2015).
16. Ge, W., Jacobs, K., Asiri, S., Foss-Feig, M. & Zubairy, M. S. Operational resource theory of nonclassicality via quantum metrology. *Phys. Rev. Res.* **2**, 023400 (2020).
17. Grangier, P., Slusher, R. E., Yurke, B. & LaPorta, A. Squeezed-light-enhanced polarization interferometer. *Phys. Rev. Lett.* **59**, 2153–2156 (1987).
18. Li, Y.-q., Guzun, D. & Xiao, M. Sub-shot-noise-limited optical heterodyne detection using an amplitude-squeezed local oscillator. *Phys. Rev. Lett.* **82**, 5225–5228 (1999).
19. Tan, K. C., Volkoff, T., Kwon, H. & Jeong, H. Quantifying the coherence between coherent states. *Phys. Rev. Lett.* **119**, 190405 (2017).
20. Yadin, B. et al. Operational resource theory of continuous-variable nonclassicality. *Phys. Rev. X* **8**, 041038 (2018).
21. Kwon, H., Tan, K. C., Volkoff, T. & Jeong, H. Nonclassicality as a quantifiable resource for quantum metrology. *Phys. Rev. Lett.* **122**, 040503 (2019).
22. Eldredge, Z., Foss-Feig, M., Gross, J. A., Rolston, S. L. & Gorshkov, A. V. Optimal and secure measurement protocols for quantum sensor networks. *Phys. Rev. A* **97**, 042337 (2018).
23. Proctor, T. J., Knott, P. A. & Dunningham, J. A. Multiparameter estimation in networked quantum sensors. *Phys. Rev. Lett.* **120**, 080501 (2018).
24. Ge, W., Jacobs, K., Eldredge, Z., Gorshkov, A. V. & Foss-Feig, M. Distributed quantum metrology with linear networks and separable inputs. *Phys. Rev. Lett.* **121**, 043604 (2018).
25. Zhuang, Q., Zhang, Z. & Shapiro, J. H. Distributed quantum sensing using continuous-variable multipartite entanglement. *Phys. Rev. A* **97**, 032329 (2018).
26. Gatto, D., Facchi, P., Narducci, F. A. & Tamma, V. Distributed quantum metrology with a single squeezed-vacuum source. *Phys. Rev. Res.* **1**, 032024 (2019).
27. Oh, C., Lee, C., Lie, S. H. & Jeong, H. Optimal distributed quantum sensing using gaussian states. *Phys. Rev. Res.* **2**, 023030 (2020).
28. Guo, X. et al. Distributed quantum sensing in a continuous-variable entangled network. *Nat. Phys.* **16**, 281–284 (2020).
29. Zhao, S.-R. et al. Field demonstration of distributed quantum sensing without post-selection. *Phys. Rev. X* **11**, 031009 (2021).
30. Xia, Y. et al. Demonstration of a reconfigurable entangled radio-frequency photonic sensor network. *Phys. Rev. Lett.* **124**, 150502 (2020).
31. Rivas, A. & Luis, A. Precision quantum metrology and nonclassicality in linear and nonlinear detection schemes. *Phys. Rev. Lett.* **105**, 010403 (2010).
32. Yu, S. Quantum fisher information as the convex roof of variance. *arXiv Preprint at* <https://doi.org/10.48550/arXiv.1302.5311> (2013).
33. Tóth, G. & Apellaniz, I. Quantum metrology from a quantum information science perspective. *J. Phys. A: Math. Theor.* **47**, 424006 (2014).
34. Scully, M. O. & Zubairy, M. S. *Quantum Optics* (Cambridge University Press, New York, 1997).
35. Tóth, G. & Petz, D. Extremal properties of the variance and the quantum fisher information. *Phys. Rev. A* **87**, 032324 (2013).
36. Braunstein, S. L. & Caves, C. M. Statistical distance and the geometry of quantum states. *Phys. Rev. Lett.* **72**, 3439 (1994).
37. Yu, H. et al. Quantum correlations between light and the kilogram-mass mirrors of ligo. *Nature* **583**, 43–47 (2020).
38. Tse, M. et al. Quantum-enhanced advanced ligo detectors in the era of gravitational-wave astronomy. *Phys. Rev. Lett.* **123**, 231107 (2019).
39. Schumaker, B. L. Quantum mechanical pure states with gaussian wave functions. *Phys. Rep.* **135**, 317–408 (1986).
40. Jacobs, K., Tittonen, I., Wiseman, H. M. & Schiller, S. Quantum noise in the position measurement of a cavity mirror undergoing brownian motion. *Phys. Rev. A* **60**, 538–548 (1999).
41. Giovannetti, V. & Vitali, D. Phase-noise measurement in a cavity with a movable mirror undergoing quantum brownian motion. *Phys. Rev. A* **63**, 023812 (2001).
42. Jacobs, K. *Quantum measurement theory and its applications* (Cambridge University Press, Cambridge, 2014).
43. Helstrom, C. W. Quantum detection and estimation theory. *J. Stat. Phys.* **1**, 231–252 (1969).
44. Qian, K. et al. Heisenberg-scaling measurement protocol for analytic functions with quantum sensor networks. *Phys. Rev. A* **100**, 042304 (2019).
45. Humphreys, P. C., Barbieri, M., Datta, A. & Walmsley, I. A. Quantum enhanced multiple phase estimation. *Phys. Rev. Lett.* **111**, 070403 (2013).
46. Knobel, R. G. & Cleland, A. N. Nanometre-scale displacement sensing using a single electron transistor. *Nature* **424**, 291–293 (2003).
47. Hoff, U. B. et al. Quantum-enhanced micromechanical displacement sensitivity. *Opt. Lett.* **38**, 1413–1415 (2013).
48. Szczykulska, M., Baumgratz, T. & Datta, A. Multi-parameter quantum metrology. *Adv. Phys. X* **1**, 621–639 (2016).
49. Gagatsos, C. N., Branford, D. & Datta, A. Gaussian systems for quantum-enhanced multiple phase estimation. *Phys. Rev. A* **94**, 042342 (2016).
50. Ciampini, M. A. et al. Quantum-enhanced multiparameter estimation in multiarm interferometers. *Sci. Rep.* **6**, 28881 EP – (2016).
51. Nichols, R., Liuzzo-Scorpo, P., Knott, P. A. & Adesso, G. Multiparameter gaussian quantum metrology. *Phys. Rev. A* **98**, 012114 (2018).
52. Gessner, M., Pezzè, L. & Smerzi, A. Sensitivity bounds for multiparameter quantum metrology. *Phys. Rev. Lett.* **121**, 130503 (2018).
53. Matsubara, T., Facchi, P., Giovannetti, V. & Yuasa, K. Optimal gaussian metrology for generic multimode interferometric circuit. *New J. Phys.* **21**, 033014 (2019).
54. Liu, J., Yuan, H., Lu, X.-M. & Wang, X. Quantum fisher information matrix and multiparameter estimation. *J. Phys. A: Math. Theor.* **53**, 023001 (2019).
55. Li, X., Cao, J.-H., Liu, Q., Tey, M. K. & You, L. Multi-parameter estimation with multimode ramsey interferometry. *New J. Phys.* <https://doi.org/10.1088/1367-2630/ab7a32> (2020).
56. Albarelli, F., Barbieri, M., Genoni, M. & Gianani, I. A perspective on multiparameter quantum metrology: From theoretical tools to applications in quantum imaging. *Physics Letters A* **384**, 126311 (2020).
57. Spagnolo, N. et al. General rules for bosonic bunching in multimode interferometers. *Phys. Rev. Lett.* **111**, 130503 (2013).
58. Wang, H. et al. Boson sampling with 20 input photons and a 60-mode interferometer in a 10^{14} -dimensional hilbert space. *Phys. Rev. Lett.* **123**, 250503 (2019).

ACKNOWLEDGEMENTS

The research of W.G. is supported by NSF Award 2243591. The research of M.S.Z. is supported by Project No. NPRP 13S-0205-200258 of the Qatar National Research Fund (QNRF).

AUTHOR CONTRIBUTIONS

W.G. and K.J. conceived this project and derived the results of the metrological power and the maximum precision. All authors wrote and reviewed the manuscript.

COMPETING INTERESTS

The authors declare no competing interests.

ADDITIONAL INFORMATION

Supplementary information The online version contains supplementary material available at <https://doi.org/10.1038/s41534-022-00670-9>.

Correspondence and requests for materials should be addressed to Wenchao Ge or Kurt Jacobs.

Reprints and permission information is available at <http://www.nature.com/reprints>

Publisher's note Springer Nature remains neutral with regard to jurisdictional claims in published maps and institutional affiliations.



Open Access This article is licensed under a Creative Commons Attribution 4.0 International License, which permits use, sharing, adaptation, distribution and reproduction in any medium or format, as long as you give appropriate credit to the original author(s) and the source, provide a link to the Creative Commons license, and indicate if changes were made. The images or other third party material in this article are included in the article's Creative Commons license, unless indicated otherwise in a credit line to the material. If material is not included in the article's Creative Commons license and your intended use is not permitted by statutory regulation or exceeds the permitted use, you will need to obtain permission directly from the copyright holder. To view a copy of this license, visit <http://creativecommons.org/licenses/by/4.0/>.

© The Author(s) 2023